Single Molecule Studies of Enzyme Mechanisms

R. Derike Smiley and Gordon G. Hammes*

Department of Biochemistry, Box 3711, Duke University Medical Center, Durham, North Carolina 27710

Received November 3, 2005

Contents

1. Introduction

The study of single molecules is a relatively new field of research but covers a wide range of systems from dilute gases to complex biological systems. A recent issue of *Accounts of Chemical Research* has been dedicated to single molecule research and provides a good starting point for exploring the scope of this field.[1] In addition, several reviews have focused on biological systems.[2−10] This review will be limited to studies of enzyme mechanisms with single molecule methods, primarily fluorescence microscopy.

What advantages do single molecule studies offer over conventional ensemble methods? Ensemble methods provide information about the average state of a large number of molecules. Dynamic fluctuations can be masked in this averaging, as can micro-heterogeneity in the sample. The observation of single molecules permits distribution functions of behavior to be developed. In terms of enzyme mechanisms, it can permit the observation of transient intermediates that may be lost in ensemble measurements. It can also distinguish between processes occurring with the single molecule of interest and interactions between reaction components in the bulk solution that are not relevant for the enzyme mechanism. Information about the dynamic coupling between protein motions and catalysis within a single molecule can be obtained. For enzymatic reactions, where multiple turnovers occur, molecules are not synchronized in their dynamic behavior, that is, at a given point in time each enzyme molecule is at a different stage of the reaction sequence. When single molecules are observed, synchronization is not an issue—the reaction sequence of each molecule can be observed. This is of particular importance for processive reactions such as DNA synthesis, as well as for a large number of other biological processes, for example, protein folding, molecular motors, and muscle action. DNA synthesis and related enzymes will be discussed in this review, but molecular motors,[11−14] actin−myosin,[14−16] intramolecular rotation in F_1 ATPases,[17] etc. are not considered. These processes are coupled to ATP hydrolysis, but the primary focus of studies with these systems has not been the mechanistic aspects of the ATPases. Also not discussed is the extensive work on ribozymes and RNA folding.[18−22]

Although only a relatively few enzyme mechanisms have been explored with single molecule methods, it is already apparent that unique information can be obtained that is difficult, or impossible, to obtain with ensemble methods. However, it should be borne in mind that even though single molecule methods represent a unique tool in the arsenal of enzymology, the results must be correlated and consistent with ensemble measurements. The elucidation of enzyme mechanisms requires a wide variety of approaches, including structure determinations, mutation analysis, chemical modifications, and kinetics.

2. Experimental Methods

This review concentrates on the use of fluorescence microscopy for studying enzyme reactions. Related methods such as atomic force microscopy, molecular tweezers, and the stretching of biological molecules through the use of magnetic beads are not considered, except for a few instances where mechanistic information has been obtained. In terms of fluorescence microscopy, the most important aspect of the experimental method is to focus the light in a very small volume to reduce the background fluorescence. This can be readily accomplished with the use of lasers and modern optical techniques.

Perhaps the most useful optical method for reducing the fluorescence background is total internal reflection (TIRF).[23] If light is passed via a prism through the sample at an appropriate angle, the light will be reflected when it encounters a change in refractive index, that is, when the light reaches the solution on the slide. A schematic representation of this experimental setup is shown in Figure 1A. For the light to be totally reflected, the angle of incidence

* Corresponding author: Phone: (919) 684-8848. E-mail: hamme001@mc.duke.edu.

10.1021/cr0502955 CCC: $59.00
Published on Web 05/27/2006

R. Derike Smiley received his B.S. degree in Agriculture from Tennessee Technological University in 1993. He received his M.S. degree (1996) and Ph.D. degree (1998) in Food Science and Technology under the direction of F. Ann Draughon at the University of Tennessee—Knoxville. In 1998, he joined the laboratory of Elizabeth E. Howell in the Department of Biochemistry, Cellular and Molecular Biology as a postdoctoral research associate. His research there focused on understanding the catalytic mechanism of the R-plasmid encoded R67 dihydrofolate reductase. In 2004, he joined the laboratory of Gordon G. Hammes in the Department of Biochemistry at Duke University Medical Center. Currently, his research is focused on applying single molecule fluorescence microscopy to the study of enzyme mechanisms.

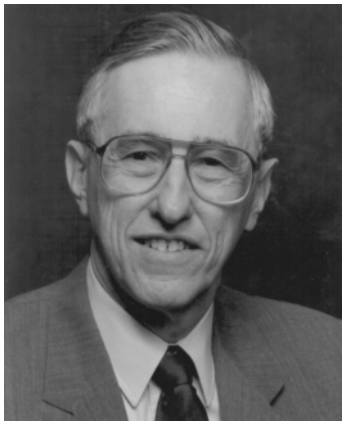

Gordon G. Hammes has held the title of Duke University Distinguished Service Professor of Biochemistry since 1996. From 1991 to 1998, he was the Vice Chancellor for Academic Affairs at Duke University's Medical Center. Dr. Hammes earned a Ph.D. from the University of Wisconsin, Madison. Upon graduation, he was an NSF Postdoctoral Fellow at the Max-Planck-Institut in Göttingen. In 1960, he joined the faculty at MIT and then moved to Cornell University in 1965 where he was chair of the Department of Chemistry (1970–1975) and Director of the Center for Biotechnology (1983–1988). From 1988 to 1991, he was the Vice Chancellor for Academic Affairs at the University of California, Santa Barbara. He is a member of the National Academy of Sciences and the American Academy of Arts and Sciences and has received several national awards, including the American Chemical Society Award in Biological Chemistry (1967) and the American Society for Biochemistry and Molecular Biology William C. Rose Award (2002). Dr. Hammes has more than 225 scientific publications, including five books. His major research interests are in biophysical chemistry, especially enzyme kinetics and mechanisms, biochemical control mechanisms, multienzyme complexes, enzyme-coupled ion transport, and single molecule fluorescence microscopy.

on the prism must exceed a critical value determined by the refractive index of the prism. Although the light is totally reflected, a low-intensity evanescent wave propagates through the solution for a very short distance. The intensity of the wave drops off exponentially with distance and typically penetrates only about 100 nm into the solution. Because of the limited penetration of the evanescent wave, a very small

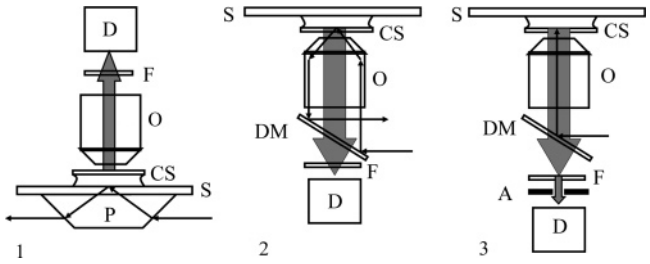

Figure 1. Schematic representation of (1) TIRF optics with a prism, (2) TIRF optics through the objective, and (3) confocal optics. In these diagrams, P is the prism, S is the slide, CS is the coverslip, O is the objective, D is the detector, F is the filter, DM is a dichroic mirror, and A is a pinhole aperture. The optical paths of the exciting light are indicated by solid arrows, whereas the emission paths are the shaded arrows.

volume at the surface of the slide is illuminated, and fluorescent molecules at the surface can be visualized even in the presence of quite large concentrations of fluorescent molecules in the solution (typically as high as 200 nM).

Commercial microscopes are available that utilize TIRF. In the commercial equipment, a prism usually is not used: instead the light is passed through a high numerical aperture objective (>1.4) at an appropriate angle, and the fluorescence is observed through the same lens. This is illustrated in Figure 1B in which the incident light is reflected through one side of the objective. By appropriate alignment of the laser, the critical angle for TIFR can be achieved, and the totally reflected light exits on the other side of the objective. The fluorescence signal is shown in the middle of the objective and passes through a filter to the detector.

Confocal optics also can be utilized, as schematically illustrated in Figure 1C. In this case, a pinhole aperture is placed in the primary image plane of the collection path of the microscope to filter out fluorescence that originates from molecules that are out of the focal plane of the objective. This effectively makes the volume of the sample that is observed very small. The primary advantage of confocal optics, in addition to the illumination of a small volume, is the ability to scan in the *z* (vertical) direction. This capability is not required for single molecule observation where the molecules of interest are confined to the surface of the slide. Traditional epiluminescence can be used to visualize single molecules, but the signal-to-noise ratio is not as high as for TIRF and confocal optics.

In practice, fluorescence microscopy can only be carried out in the visible region of the spectrum. Typical lasers include relatively inexpensive tunable Ar lasers and diode pumped double YAG lasers. High power is not required: 10 mW is usually more than enough.

Two methods are used for observation of the signal: an avalanche photodiode, APD (available only from Perkin-Elmer), or a high-quality CCD, ICCD or EMCCD camera. The APD has the advantage of counting single photons at a very high efficiency with a very low dark count, but the APD does not have spatial resolution so that only one molecule at a time can be observed. The active area of an APD is very small so that the density of single molecules can be readily adjusted so as to observe only a single molecule. The camera has the advantage of observing multiple single molecules simultaneously, but the signal-to-noise ratio is not as good as the APD and the practical time resolution is limited to about 10 ms. In contrast, microsecond times (or faster in principle) can be observed with an APD. The time

resolution of single molecule experiments is not only limited by the time response of the detector. The relatively small number of photons emitted per unit time by single molecules also is a limitation. At very short times, the number of photons may be too few to detect. The two methods of observation are complementary: both methods may be required to carry out a complete study of an enzymatic system.

The time course (trajectory) of individual molecules can be observed directly with the APD when the APD is interfaced to a computer. With cameras, timed sequences of photos are taken, and computer programs such as NIH Image (http://rsb.info.nih.gov/nih-image/) are used to analyze the data and to create trajectories for individual molecules.

Two modes of fluorescence detection have primarily been used. For a single fluorescent probe, changes in the fluorescence can be monitored directly through the use of appropriate filters in the microscope. Fluorescence resonance energy transfer (FRET) also can be a useful measure of reaction progress. In this case, microscope filters can be used to monitor the fluorescence of the donor, FRET, and direct excitation of the acceptor. For the observation of FRET, the fluorescence signal can be split with a dichroic mirror, and donor and acceptor fluorescence can be monitored simultaneously through the use of appropriate filters. For quantitative analyses of FRET experiments, spectral overlaps of donor and acceptor need to be taken into account.

3. Sample Preparation

Initial efforts to visualize single molecules in biological systems utilized the technique of fluorescence correlation spectroscopy in which a small number of molecules were observed in a flow cell.[24] This technique primarily provides information about the diffusion of single molecules although information about other processes also can be obtained as an addition to the diffusion equations used to interpret the data. To study enzymatic reaction mechanisms optimally, it is necessary to restrict the enzyme to the surface of the slide. Most importantly it is essential that this restriction to the surface not cause heterogeneity in the sample and that the enzyme has its full activity. Enzyme activity should be measured in situ. The detection of heterogeneity is more difficult—this requires looking at a large number of different molecules, looking at a single molecule undergoing a large number of reactions, or both. Even then, assessing whether heterogeneity is due to sample preparation or is intrinsic for the enzyme is difficult.

A variety of different methods have been use for immobilization. The first studies with enzymes were done by putting the enzyme into agarose or similar gels.[25] This places the enzyme in a restricted volume that may alter its activity. Probably the best method is to use tethering whereby the enzyme is attached to the slide via an extended "arm". The most common method of doing this is to make use of the biotin−avidin interaction, which has a binding constant of about 10^{15} M^{-1}. For example, a glass slide can be silanized to give a surface of free amino groups. The amino groups can then be biotinylated with a succinimide ester of biotin and avidin is then added.[26] An arm having biotin at the end can be attached to one of the termini of the enzyme and interacted with the avidin on the slide. The enzyme is very effectively immobilized but is sufficiently far from the surface so that it can have its normal solution properties. Several variations of the biotin−avidin interaction have been utilized; for example, biotinylated bovine serum albumin can be attached to the slide through nonspecific surface interactions, followed by avidin and the biotinylated enzyme.[27] For enzymes that utilize DNA as a substrate, it is very easy to obtain biotinylated DNA, which can be tethered to the slide. As previously mentioned, optical tweezers[6,9] and magnetic beads[6] are also effective tethering devices.

The concentrations of fluorescent proteins/nucleic acids required are very low, typically in the nanomolar to picomolar range. Even with very low concentrations, nonspecific binding of proteins/nucleic acids to the glass surface can cause a high fluorescence background. Very often an inert protein, for example, bovine serum albumin ($\sim$10 μM), is added to solutions to eliminate nonspecific binding.[26] Treatment with poly(ethylene glycol) also is useful for this purpose because it creates a hydrophilic surface.[28]

The most difficult task of all is to insert a fluorescence probe on the enzyme that monitors the process of interest and does not alter the enzyme activity significantly: no formula exists for doing this. Both direct observation of fluorescence and FRET have been used for this purpose. The FRET can be between two probes on a single enzyme molecule or between a probe on the enzyme and an exogenous molecule. Specific examples of both situations are discussed below. Parameters other than changes in fluorescence also can be utilized, for example, translational displacement of kinesin on microtubules[7,8] and translational movement of enzymes on DNA and RNA.[29,30] Measurements of fluorescence polarization also are useful to determine the rotational mobility of the fluorescent probe.[25,31]

In selecting fluorescence probes, it should be borne in mind that photobleaching occurs quite readily in single molecule experiments. Thus fluorescein is not a good probe—in our equipment the half time for photobleaching is about 6 s. Alexa dyes, on the other hand, are much more stable with half-times in the 20−30 s range. Cy dyes also have been extensively used. The occurrence of photobleaching is probably the easiest check to be certain single molecules are being observed. For single molecules, photobleaching is an all or none process, that is, it occurs in one step rather than by increments whereby the fluorescent spot becomes dimmer and dimmer. Furthermore, photobleaching of a population of single molecules should be an exponential process. Photobleaching can be reduced with oxygen scavenging systems such as glucose oxidase, but this adds additional components to the system.[32]

4. Theory of Single Molecule Reactions

The kinetics of single molecule transitions differs from ensemble measurements in that a distribution of time constants is observed as the molecule goes back and forth between states. The distribution of time constants, that is, reaction lifetimes, can be related to the ensemble rate constants for specific mechanisms. Only two simple examples are discussed here. The single molecule kinetics of more complex mechanisms, including an extended Michaelis−Menten mechanism, have been developed.[33−35]

The development of the kinetic equations follows the procedures of conventional kinetics except that rather than concentration, the probability of a given state is used. Consider, for example, the one-step mechanism

$$A \xrightarrow{k} B \qquad (1)$$

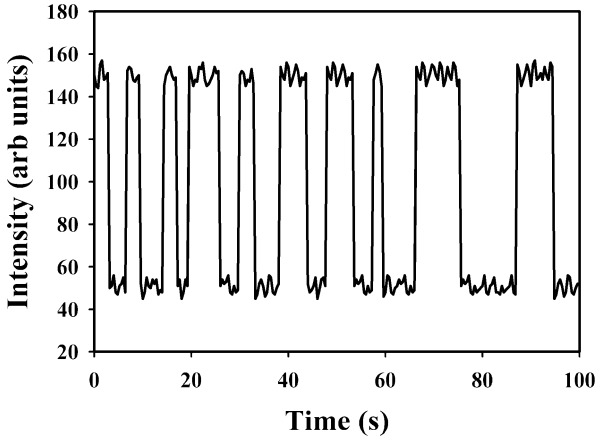

Figure 2. Hypothetical trajectory for a single molecule going between high and low fluorescence states. The fluorescence versus time is plotted.

where k is the ensemble rate constant. The rate equation for a single molecule going from state A to state B is given by

$$dP_A/dt = -kP_A \quad (2)$$

Here P_A is the probability of the molecule being in state A and t is the time. This equation can be solved with the initial condition that $P_A = 1$ when $t = 0$, and $P_A = P_A$ when $t = \tau$, the reaction lifetime. The result is

$$P_A = \exp(-k\tau) \quad (3)$$

Thus for this simple mechanism the probability distribution of lifetimes follows an exponential function, and the ensemble rate constant is directly related to this distribution.

The probability density, $f(\tau)$, is defined by the relationship $-dP_A/d\tau = kP_A = f(\tau)$ or

$$f(\tau) = k \exp(-k\tau) \quad (4)$$

Note that $f(\tau)\, d\tau$ is the probability of A switching to B during the interval τ and $\tau + d\tau$. The distribution function $f(\tau)$ is determined experimentally in single molecule studies. How does this work in practice? In Figure 2, a schematic representation of the trajectory of a molecule is shown as the molecule goes from a high to a low fluorescent state. The reaction lifetimes can be tabulated from such trajectories, and the probability density of the lifetime falling within a given range can be plotted as a bar graph as shown in Figure 3. The probability density is simply the number of events with a lifetime τ, $N(\tau)$, divided by the total number of events, N_{total}. Practical considerations require the use of bar graphs with significant bar widths because only a few hundred lifetimes are generally tabulated.

As a second example, consider the simple two-step reaction

$$\underset{\text{high}}{\text{A}} \xrightarrow{k_1} \underset{\text{high}}{\text{B}} \xrightarrow{k_2} \underset{\text{low}}{\text{C}} \quad (5)$$

The fluorescent state of the molecule is indicated by high or low fluorescence. In this case,

$$-dP_A/dt = k_1P_A \quad (6)$$

$$-dP_B/dt = k_2P_B - k_1P_A \quad (7)$$

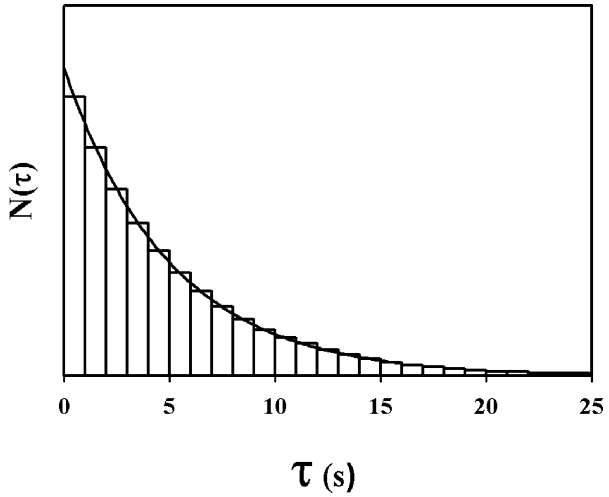

Figure 3. Histogram of the number of events with a lifetime τ, $N(\tau)$, versus τ for the lifetimes of a single molecule moving from a high fluorescence state, A, to a low fluorescence state, B (eq 1). The line has been calculated with eq 4 and $k = 0.2\ s^{-1}$.

If $P_A = 1$ and $P_B = P_C = 0$ when $t = 0$, then when $t = \tau$,

$$P_A = \exp(-k_1\tau) \quad (8)$$

$$P_B = [k_1/(k_2 - k_1)][\exp(-k_1\tau) - \exp(-k_2\tau)] \quad (9)$$

The probability density for the high fluorescent state in this case is

$$f(\tau) = k_2P_B = [k_1k_2/(k_2 - k_1)][\exp(-k_1\tau) - \exp(-k_2\tau)] \quad (10)$$

These equations predict that the distribution of reaction lifetimes for the high fluorescence state should be described by the difference between two exponentials. This has been observed for the enzyme cholesterol oxidase, as will be discussed later.[25] This behavior will be observed only when an enzyme cycles between two states during steady-state catalysis with an essentially irreversible step in the cycle.

In general, when a specific enzyme is considered, it is useful to generate the reaction lifetimes predicted by the mechanism. A computer program has been developed for this purpose.[36]

Alternative methods of analyzing trajectories are used such as correlation and autocorrelation functions. These more mathematical approaches provide direct information about the time scale of events that occur and can reveal the occurrence of multiple processes, as well as whether reaction events are random or correlated with previous events. However, the link to mechanism is somewhat more indirect than a reaction lifetime analysis.

5. Flavin Enzymes

5.1. Cholesterol Oxidase

The first detailed study of an enzyme using single molecule fluorescence microscopy was of cholesterol oxidase,[25] although enzymatic turnovers related to motor proteins were observed earlier.[11−14] Cholesterol oxidase catalyzes the oxidation of a ring hydroxyl to a ketone by molecular oxygen with FAD as a cofactor. An enzymatic cycle involves the reduction of fluorescent FAD to nonfluorescent $FADH_2$, thus providing a built-in fluorescent indicator of the reaction

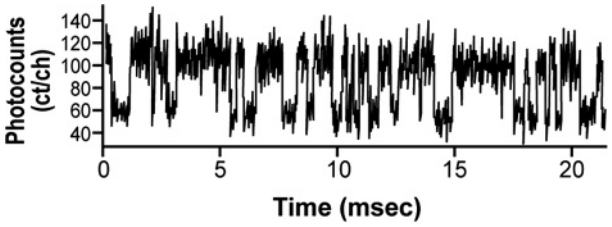

Figure 4. Trajectory for a single molecule of cholesterol oxidase alternating between a fluorescent flavin, FAD, and a nonfluorescent flavin, $FADH_2$, according to eq 11. The fluorescence emission (counts/channel) is plotted versus the time. Reprinted with permission from X. S. Xie and H. P. Lu *J. Biol. Chem.* **1999**, *274*, 15967−15920. Copyright 1999 American Society for Biochemistry and Molecular Biology.

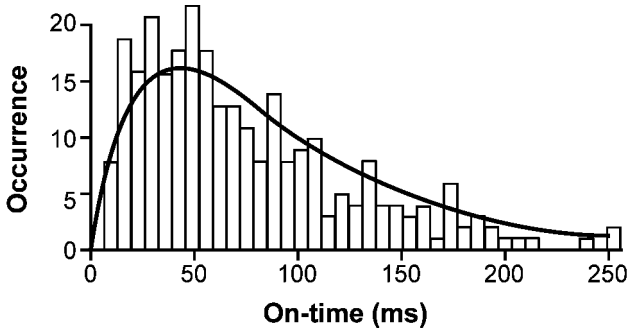

Figure 5. Distribution of the reaction lifetimes for the high fluorescence state (FAD) of cholesterol oxidase. A histogram of the number of events with a lifetime τ is plotted versus τ. The line has been calculated according to eq 10 with $k_1 = 33\ s^{-1}$ and $k_2 = 17\ s^{-1}$. Reprinted with permission from X. S. Xie and H. P. Lu *J. Biol. Chem.* **1999**, *274*, 15967−15920. Copyright 1999 American Society for Biochemistry and Molecular Biology.

progress. The single molecules of cholesterol oxidase were confined to the surface of the slide in an agarose gel of 99% water. Polarization measurements indicated that the molecules were freely rotating within the gel. Moreover, ensemble assays of the enzyme/gel mixture indicated that the turnover numbers were similar to those in aqueous solution. The substrate molecules, cholesterol and oxygen, diffuse freely in and out of the gel.

Figure 4 shows the fluctuation of fluorescence for a single enzyme molecule due to the oxidation−reduction of the flavin through successive enzyme cycles. The mechanism for this reaction can be written as

$$\mathrm{E{-}FAD} + \mathrm{S} \underset{k_{-1}}{\overset{k_1}{\rightleftharpoons}} \mathrm{E{-}FAD{-}S} \xrightarrow{k_2} \mathrm{E{-}FADH_2} + \mathrm{P} \quad (11)$$

$$\mathrm{E{-}FADH_2} + \mathrm{O_2} \rightleftharpoons \mathrm{E{-}FADH_2{-}O_2} \rightarrow \mathrm{E{-}FAD} + \mathrm{H_2O_2} \quad (12)$$

The distribution of reaction lifetimes for the high fluorescence state (FAD) obtained from the trajectories of single molecules is shown in Figure 5. This behavior is consistent with eqs 9 and 10. This can be understood in terms of the enzymatic reaction if the reaction observed is eq 11 with $k_{-1} \approx 0$. The line in the figure has been calculated with eq 10 and the rate constants given in the figure legend. As expected, k_1 increases as the concentration of cholesterol increases, whereas k_2 is relatively constant.

A detailed analysis of k_2 was carried out for different molecules with the substrate 5-pregen-3β-20α-diol (a cholesterol analog) at a concentration of 2 mM. The results obtained indicate that heterogeneity exists in the value of this rate constant for different molecules: values between 3 and 14 s^{-1} were obtained. This heterogeneity was attributed to the relatively slow interconversion of two states of the enzyme having different characteristic values of k_2. The discovery of dynamic heterogeneity, that is, that the catalytic rate constant of a single enzyme molecule is not constant but fluctuates with time, is unexpected. The molecular basis for this finding and its significance for physiological systems are not fully understood. The Michaelis−Menten mechanism can accommodate the dynamic heterogeneity observed in single molecule experiments.[25,35] This study is significant in demonstrating that unique mechanistic features of enzymatic reactions can be revealed by single molecule measurements.

In a related work, the quenching of FAD fluorescence bound to flavin reductase from *Escherichia coli* by a nearby tyrosine residue was studied.[37] This quenching is due to photoinduced electron transfer. The experimental observation is that a distribution of fluorescence lifetimes (nanoseconds) is observed with ensemble measurements. Even for a single molecule, the fluorescence decay does not follow the time dependence of a single exponential. This nonexponential behavior is attributed to a dynamic distribution of lifetimes. The distribution of lifetimes and fluorescence quenching by tyrosine can be characterized by an autocorrelation function that suggests the protein motions responsible for the fluorescence lifetime fluctuations extend from hundreds of microseconds to seconds. The derived autocorrelation function is a complex mathematical interpretation of the experimental results. Nevertheless, the possibility that a wide range of enzyme motions may be involved in reactivity is intriguing.

5.2. Dihydroorotate Dehydrogenase

The enzyme dihydoorotate dehydrogenase from *E. coli* is an FMN-requiring enzyme that oxidizes dihydoorotate to orotate. It is a membrane-bound enzyme, and the reaction can be conveniently divided into two half-reactions. In the first half-reaction, dihydroorotate reduces FMN, forming orotate. In the second half-reaction, the reduced enzyme−orotate complex binds a quinone substrate, FMN is oxidized, and the products are released. As with cholesterol oxidase, the kinetics can be conveniently monitored through the fluorescence of the flavin. In the single molecule study, the enzyme was confined to the surface in the pores of a 1% agarose gel.[38] Following the addition of substrates, flavin blinking could be observed until the flavin dissociated from the enzyme, resulting in an abrupt loss of fluorescence.

In the absence of flavin dissociation, the fluorescence-on reaction time distribution for 50 molecules could be fit to two exponentials (4 s^{-1} and 0.9 s^{-1}). The fluorescence-off reaction time distribution did not display this heterogeneity. When 0.1% Triton X-100 is added, a similar biphasic distribution is observed but with increased rate constants. Similar results were obtained with stopped flow experiments. Consequently, these differences are attributed to static heterogeneity. Further analysis of the data indicates that the heterogeneity of the sample is decreased as detergent is added, with the ensemble rate constant increasing as the detergent concentration increases. Thus the static heterogeneity in this case may be an artifact of the preparation, although the authors suggest this may have physiological implications. No dynamic disorder was revealed in the reaction rates by an autocorrelation analysis of the data. In this case, the single molecule technology permits direct observation of the flavin,

and the results are nicely correlated with ensemble measurements. However, the results are ambiguous with respect to whether heterogeneity in the reaction rates is physiologically relevant.

5.3. *p*-Hydroxybenzoate Hydroxylase

The enzyme *p*-hydroxybenzoate hydroxylase is representative of a family of flavoprotein monooxygenases. It is a homodimer, and each subunit binds one molecule of FAD. This enzyme is important because it modulates physiological reactions of oxygen. A single-molecule study of this enzyme was carried out to determine the conformational states of the enzyme, particularly with regard to flavin binding.[39] Again, the enzyme was confined to the surface of the slide in an agarose gel, and "blinking" of the flavin was observed. This blinking was attributed to the flavin moving between two conformations: an open conformation in which the flavin is exposed to solvent, and an in conformation in which it is more buried into the protein. The fluorescence state is attributed to the open conformation and the nonfluorescent state to the in conformation. Moreover, the in conformation is postulated to be the form that binds the substrate during catalysis.

For the wild-type enzyme, 55% of the enzyme molecules did not display blinking—instead the fluorescence was constant until the flavin dissociated and fluorescence was lost. For the other molecules, the reaction time distribution could be fit to a single exponential with rate constants of 6.4 and 21 s^{-1} for the open-to-in and in-to-open conversions, respectively. These rates and the equilibrium constants are different for mutant enzymes. For one of the mutant enzymes examined, a biexponential fit of the reaction time distribution was required, suggesting additional heterogeneity.

The results obtained from this work clearly suggest dramatic static heterogeneity in the conformation of the enzyme−flavin complex and possible dynamic heterogeneity on the second time scale. However, it should be noted that the majority of the data were obtained with a single FAD bound to the dimeric enzyme. Limited data obtained for the enzyme in which two FAD are bound suggest fluctuation between a state in which both flavins are in the open configuration and a state in which one flavin is in an open configuration and one in an in configuration. These results demonstrate the power of single molecules being able to distinguish between different reactivities of individual molecules and suggest significant heterogeneity in the reaction rates. The role of these multiple conformations in the reaction cycle remains to be clarified, perhaps by a single molecule study of the overall reaction.

6. Staphylococcal Nuclease

Single molecule FRET was used to characterize conformational dynamics and the cleavage mechanism of staphylococcal nuclease.[31] This well-characterized enzyme catalyzes the hydrolysis of DNA and RNA into mono- and dinucleotides. Two types of experiments were carried out: one examined intramolecular FRET between two fluorescent entities on a single enzyme molecule whereas the other looked at intermolecular FRET between an enzyme with a single donor fluorophore and an acceptor-labeled DNA substrate. The enzyme was tethered to the glass coverslip by use of a silanizing reagent that provided a surface of ethylenediamine triacetic acid. A hexahistidine tag was added to the enzyme and Ni^{2+} was used to attach the enzyme to the coverslip. A specific cysteine on the enzyme was labeled with tetramethylrhodamine, the fluorescence energy donor. A doubly labeled enzyme was constructed by further labeling of the enzyme with Cy5 succinimidyl ester. Approximately 15−20% of the enzyme was doubly labeled, but it is very likely that heterogeneity existed with regard to the specific amino group labeled. The DNA substrate was specifically labeled at either the 3′ or 5′ end with Cy5.

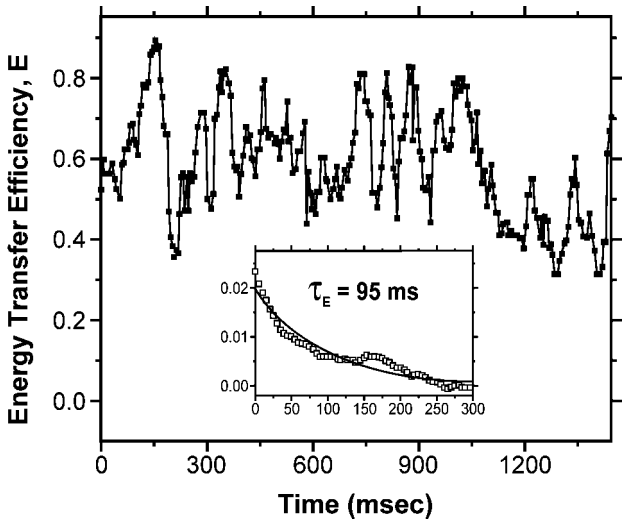

Figure 6. Plot of the FRET efficiency versus time for single molecules of double labeled staphylococcal nuclease. The inset shows the autocorrelation of the data that suggests a time scale of 95 ms for the conformational fluctuations. Reprinted with permission from T. Ha, A. Y. Ting, A. Y. Liang, W. B. Caldwell, A. E. Deniz, D. S. Chemal, P. G. Schultz, and S. Weiss *Proc. Natl. Acad. Sci. U.S.A.* **1999**, *96*, 893−898. Copyright 1999 National Academy of Sciences U.S.A.

Single molecules of the tethered double labeled enzyme were monitored by measuring the time dependence of the fluorescence for both the acceptor and donor. Fluctuations of the fluorescence on the millisecond time scale were found for both signals. A typical result is shown in Figure 6 where the FRET is plotted versus time. The distribution of reaction lifetimes obtained from trajectories such as this is shown in Figure 7. Unfortunately the interpretation of these results is difficult because of the heterogeneity of the amino group labeling, which can result in somewhat different kinetic processes for each molecule. This work convincingly demonstrated, however, that the fluctuations in fluorescence are due to FRET and not to alterations in the rotational properties of the probes. This was done by measuring the rotational mobility of the probes. These results indicate that the structure of the enzyme is fluctuating between multiple conformations on the millisecond time scale. If an inhibitor of the enzyme is added, fluctuations still occur but with a longer time constant, suggesting that the binding of an inhibitor reduces the conformational mobility of the protein.

The interaction of a fluorescent DNA substrate with the enzyme was studied by flowing the substrate past the tetramethylrhodamine labeled enzyme. The fluorescence of the enzyme was monitored and was found to fluctuate with time as the substrate flowed past. A modified enzyme with a reduced turnover number was used for these experiments to make enzyme reaction events observable within the accessible time scale of the experiments. The lifetime of the substrate−enzyme reaction could be directly determined from the time course of the donor fluorescence. The distribution

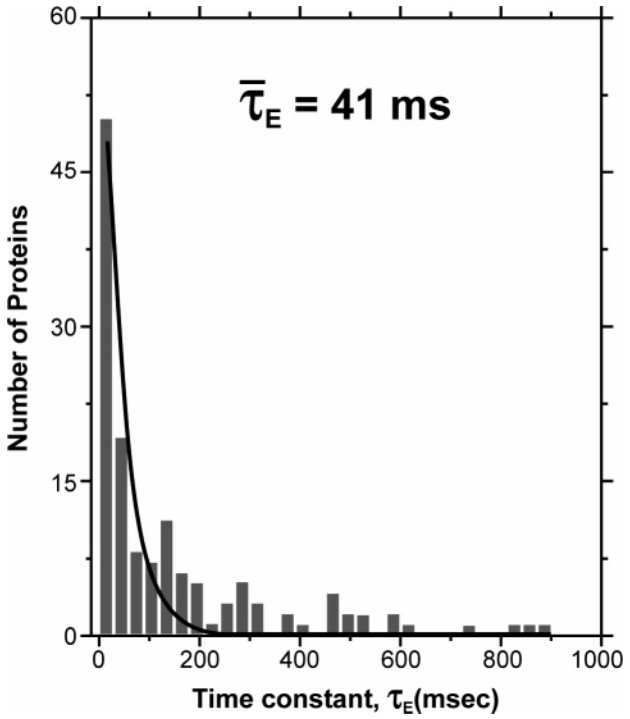

Figure 7. Distribution of reaction lifetimes for single molecules of double labeled staphylococcal nuclease obtained from trajectories such as that shown in Figure 6. The number of proteins with a reaction lifetime τ is plotted versus τ. The average value of τ is 41 ms. The line is a single-exponential fit of the data. Reprinted with permission from T. Ha, A. Y. Ting, A. Y. Liang, W. B. Caldwell, A. E. Deniz, D. S. Chemal, P. G. Schultz, and S. Weiss *Proc. Natl. Acad. Sci. U.S.A.* **1999**, *96*, 893−898. Copyright 1999 National Academy of Sciences U.S.A.

of time constants could be approximated by a single exponential. The mechanistic step characterized by this time constant cannot be ascertained. It could be single bond cleavage of DNA, multiple and successive cleavages, binding and unbinding of substrate, and/or nonspecific interactions. In addition, photobleaching is a significant problem in these experiments. The results clearly indicated, however, that the characteristic time constant for enzyme−substrate association is significantly faster for 3′ labeled substrate than for 5′ labeled substrate. A possible interpretation of these results is that the 3′ to 5′ cleavage is processive (the 5′ end remains bound) whereas the 5′ to 3′ cleavage is not processive. Although questions remain about the mechanistic interpretation of the experimental results, these results demonstrate that unique mechanistic information can be obtained from single molecule experiments.

7. Dihydrofolate Reductase

Dihydrofolate reductase (DHFR) catalyzes the NADPH-dependent hydride transfer reaction to form tetrahydrofolate from dihydrofolate. Tetrahydrofolate is essential in the biosynthesis of thymidylate, methionine, purine nucleotides, and other metabolites. Inhibition of DHFR arrests DNA synthesis and cell division and results in cell death. Chromosomal DHFR has therefore become the target for antifolate drugs in the treatment of cancer and bacterial infections. Methotrexate is a clinically important drug for the inhibition of human chromosomal DHFR during cancer treatment.

Single molecule fluorescence microscopy was used to monitor a conformational change associated with methotrexate binding to DHFR.[26] Methotrexate binds very tightly to DHFR with a dissociation constant of approximately 10 nM. DHFR was attached to an aminosilanized slide via a biotin−avidin−biotin bridge. The tethered DHFR was assayed in situ and found to be fully active. A specific cysteine (amino acid position 18) of DHFR was labeled with AlexaFluor 488. A Pentamax ICCD camera was then used to observe the fluorescence of the AlexaFluor 488 both in the presence and in the absence of methotrexate.

Fluctuations in fluorescence intensity between two well-defined states were observed in the presence of methotrexate but not in its absence. The ensemble average rate constants were obtained from the distribution of reaction lifetimes that were adequately described by a single exponential (eq 4). Fluorescence quenching is not directly related to the association−dissociation process since the ensemble average rate constants are much larger than the rate constant for dissociation of methotrexate from its complex with DHFR (0.02 s^{-1}). The fluctuation in fluorescence intensity was attributed to a conformational change involving the opening and closing of the Met20 loop over the methotrexate.

Subsequent single molecule experiments investigated the binding of the individual natural substrates, NADPH and dihydrofolate, to DHFR.[40] As with methotrexate, fluctuations in fluorescence intensity between discrete states were only observed in the presence of substrate. In all cases, the distributions of lifetimes were adequately described by a single exponential from which the ensemble average rate constants were obtained. This process can be represented as

$$\text{high intensity} \underset{k_r}{\overset{k_f}{\rightleftharpoons}} \text{low intensity} \qquad (13)$$

where k_f and k_r are the ensemble average rate constants.

In the case of dihydrofolate, k_f was found to be concentration dependent, and the concentration dependence suggested that a conformational change following binding is being observed. The rate constant k_r was found to be concentration independent, with a value of approximately 5 s^{-1}. As with methotrexate, the conformational change is attributed to movement of the Met20 loop. When NADPH was the reactant, k_f also was concentration dependent whereas k_r was concentration independent, with a value of approximately 4 s^{-1}. In this case, k_f increased linearly with the concentration of NADPH, indicating that a bimolecular reaction was being observed, and k_r is the rate constant for dissociation of NADPH from the enzyme. The second-order rate constant for the binding reaction was determined to be 2.6×10^6 M^{-1} s^{-1}. The equilibrium dissociation constant calculated from the rate constants, 1.4 μM, is in good agreement with that determined by fluorescence titration, 1.5 μM. Stopped-flow ensemble experiments also were carried out and correlated with the single molecule experiments.

Single molecule experiments were conducted to measure fluorescence quenching in the presence of an equilibrium mixture of substrates to monitor the interconversion of reaction intermediates.[40] For these experiments, the trajectories of single molecules with lifetimes <100 ms were followed with an APD. In the presence of an equilibrium mixture of substrates, fluctuation of the fluorescence intensity between two discrete states was observed. Fluctuations between discrete states were not observed in the absence of substrates. The results were analyzed assuming two states, high and low fluorescence. The ensemble average rate constants obtained from a single-exponential fit of the

lifetime distributions were 168 and 473 s^{-1} for k_f and k_r, respectively. The single molecule experiment was repeated substituting NADPD for NADPH, and the corresponding values of k_f and k_r were found to be 73 and 494 s^{-1}. The isotope rate effect (>2) for k_f suggests that hydride transfer is being observed. The unidirectional isotope rate effect that was observed may be indicative that the single exponential deconvolution of the data is an oversimplification and that a multiexponential fit is needed. Unfortunately, the time resolution of the equipment and relatively low signal-to-noise ratio are insufficient to resolve multiexponentials. It is therefore likely that the rate constants k_f and k_r are not rate constants for the same single step.

To relate the dynamics of DHFR to distance changes between residues, DHFR was labeled at amino acid position 37 with Alexa 555 and at amino acid position 17 with the fluorescence quencher QSY 35.[41] The distance between the probes was such that approximately 50% FRET was observed. The double labeled DHFR was attached to glass coverslips as in previous single molecule DHFR experiments, and FRET was monitored with an APD. Fluctuations in fluorescence intensity between two discrete states were observed in the presence of an equilibrium mixture of substrates but not in their absence. Similar fluctuations in fluorescence intensity were not observed when either NADPH or DHF was present individually. The distributions of reaction lifetimes observed were not entirely consistent with a single exponential function, apparently because of the undercounting of short lifetimes. If the shortest lifetimes are not included, a single exponential describes the data well, with ensemble average rate constants of approximately 200 s^{-1} at pH 8.5. A kinetic isotope effect was not observed when NADPH was substituted for NADPD. Stopped-flow ensemble experiments indicated the occurrence of a conformational change with a similar rate constant and no isotope rate effect.

A mutated enzyme with greatly reduced catalytic activity (G121V) also was studied. This mutation is quite distant from the active site. The ensemble average rate constants were slightly reduced, suggesting that the conformational change is linked to hydride transfer, although not directly.

The dependence of fluorescence energy transfer on the distance between the two probes is given by

$$\frac{F_\infty - F}{F_\infty} = \frac{1}{1 + (R/R_0)^6} \tag{14}$$

where F_∞ is the fluorescence intensity of the donor at infinite distance, F is the observed fluorescence, R is the distance between probes, and R_0 is the distance at which 50% energy transfer occurs. For the probes used, $R_0 = 24$ Å and the X-ray structure of DHFR suggests that $R \approx 28$ Å. The total differential of eq 14 with F and R as variables is

$$\frac{\Delta F}{F_\infty - F} = \frac{6(\Delta R/R)}{1 + (R_0/R)^6} \tag{15}$$

If the observed changes in FRET are attributed solely to distance changes between the probes, the distance change between the two probes in going from the high to low fluorescence states was estimated to be 1−2 Å. Calculation of this distance assumes that the observed fluorescence change is entirely due to a change in distance between the backbone sites rather than to environmental changes with regard to the fluorescent probe. In support of this interpretation, the fluorescence probe rotates relatively freely, as suggested by anisotropy measurements, on a time scale much faster than the reaction, and the transitions between fluorescence states are observed only when $R \approx R_0$. Thus, this is probably a reasonable estimate of the distance change. Theoretical calculations have suggested that distance changes of individual residues in the 1 Å range are associated with the hydride transfer reaction.[42] These results are consistent with the idea that very small conformational changes are involved in the modulation of enzyme catalysis.

Single molecule fluorescence studies have revealed subtle roles for conformational fluctuations in the catalytic mechanism of DHFR. Future studies are planned to map distance changes throughout the DHFR molecule by placing FRET pairs at strategic locations away from the active site. The results obtained may be useful in elucidating questions concerning the coupling of conformational changes throughout the enzyme molecule to catalysis.

8. Conformational Heterogeneity

Conformational heterogeneity has been found in the studies of cholesterol oxidase, flavin reductase, dihydrooroate dehydrogenase, *p*-hydroxybenzoate hydroxylase, and staphylococcal nuclease, as previously discussed. Similar but less well-defined results have been observed with other enzymes.

The conformational dynamics of single molecules of bacteriophage T4 lysozyme have been examined by labeling the protein with Texas Red and tetramethylrhodamine at locations that can monitor hinge bending motions through changes in FRET.[43] In this case, the enzyme was attached to a silanized slide through a bifunctional linker. In the absence of substrates, an autocorrelation analysis of fluorescence trajectories suggested that the enzyme fluctuates between multiple conformations (dynamic heterogeneity?) and that static inhomogeneity also exists.

The fluorescence trajectories also were determined in the presence of a substrate, namely, a sonicated *E. coli* cell wall. With such a complex system, it is not surprising that the overall enzymatic reaction rate constants varied greatly for individual molecules. The data suggested that the dominant contribution to this static inhomegeneity is the enzyme searching for reactive sites on the substrate and that subsequent steps in the catalysis have homogeneous rates among the individual molecules. Furthermore, the mechanism involves multiple intermediates in the formation of the active enzyme−substrate molecule. Although this mechanism is consistent with the data, some of the observed heterogeneity may be due to the method of attachment of the enzyme to the slide and the complex substrate used.

The single molecule kinetics of lipase B from *Candida antartica* has been studied using a substrate that produces a highly fluorescent product.[44] The enzyme was attached to the slide by creating a hydrophobic surface and allowing the enzyme to bind to this surface. The enzyme was visualized by nonspecific labeling with Alexa 488. Once the enzyme was located, the Alexa 488 was photobleached before adding the substrate. Although the enzyme is active after this treatment, it should be recognized that nonspecific hydrophobic binding as an attachment method is almost certain to produce static heterogeneity with respect to the conformation of the enzyme. Furthermore, the presence of various amounts of bleached Alexa 488 on the enzyme also produces

heterogeneity. Thus static heterogeneity is inherent in this experiment.

When substrate was added to the lipase bound to the slide, a "blinking" of the fluorescence was observed as the production of successive product molecules was observed. An analysis of the time dependence of the blinking times indicated that the process underlying the catalysis could not be described by a single rate constant, i.e, a single exponential was not adequate to describe the distribution of reaction times. A model was developed that postulated conformational interconversions of an enzyme on the same time scale as the catalytic reaction. A more extensive examination of this system is needed to sort out the individual steps, but some type of conformational heterogeneity, both dynamic and static, appears to occur for this system.

One of the first single molecule studies of conformational dynamics of an enzyme was with horseradish peroxidase.[45] The enzyme was fixed to the slide via the biotin/avidin interaction, and a substrate was used that produced a fluorescent product. Correlation and autocorrelation functions were used to analyze the fluctuations of the fluorescence that occurred. A single enzyme molecule was found to fluctuate in its catalytic activity over a wide range of time scales. The mechanism suggested by the data is that a large distribution of rates exists for the formation of the enzyme−product complex, but the dissociation of product from the enzyme is described by a single exponential. The data analysis is quite complex, but the occurrence of static and dynamic heterogeneity again is a feature of the interpretation of the observations. Further studies are needed to characterize this system more definitively.

A conceptual model has been proposed that is instructive for understanding the role of conformational changes in catalysis and possible differences that may be encountered between ensemble and single molecule experiments.[35,41] In this model, a protein can be viewed as existing in multiple conformations, a view often used in the field of protein folding. The various enzyme−substrate complexes on the reaction pathway can then be viewed as interconverting conformations. The rate of catalysis associated with each catalytically competent conformation may be different. The reaction sequence then consists of a series of reaction intermediates leading to catalysis, with each reaction intermediate present in multiple conformations. Schematically this can be represented as

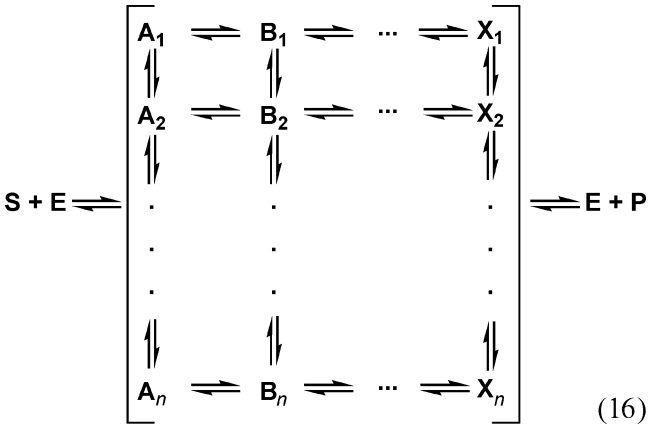

(16)

For simplicity, the multiple conformations of E are not shown and only a single substrate, S, and product, P, are shown. The A_i, B_i, C_i, etc. represent conformations of enzyme−substrate complexes that are in the catalytic pathway, and parallel catalytic pathways exist, $A_1 \rightarrow B_1 \rightarrow ... \rightarrow X_1$, etc.

If the conformations of A_i, B_i, etc. equilibrate rapidly relative to the rates of interconversion of reaction intermediates, then the catalysis proceeds by a single reaction: $\sum A_i \rightarrow \sum B_i \rightarrow ... \rightarrow \sum X_i$. In this case, only the average conformation of each reaction intermediate can be observed experimentally. On the other hand, if the conformations of A_i, B_i, etc. equilibrate slowly relative to the rates of interconversion of intermediates along the reaction pathway, catalysis essentially occurs through independent catalytic pathways. At the single molecule level, this will be observed as static heterogeneity (or dynamic heterogeneity if the equilibration is fast relative to the observation time.) At the ensemble level, the observed rates would be an appropriately weighted average of the flux through each pathway, and distinguishing multiple reaction pathways is difficult. For the intermediate case, in which the vertical and horizontal steps have comparable rates of equilibration, dynamic heterogeneity would be observed in single molecule experiments. (This implies, of course, that the rate of equilibration along both vertical and horizontal pathways is rapid relative to the time scale of the experiment.) It is unlikely these multiple pathways would be distinguished in ensemble experiments. This conceptual model, probably oversimplified, is useful for thinking about the role of conformational changes in enzyme catalysis, as well as possible differences in the experimental observations for ensemble and single molecule experiments.

Single molecule experiments have shown the existence of both static and dynamic heterogeneity. The physiological relevance of the findings remains to be elucidated. In addition, the contribution of the special microenvironment at the slide surface to the observed phenomenon is unknown. In terms of future work, careful attention needs to be paid to attaching molecules to the slide surface so that attached molecules have the same behavior and microenvironment as those in bulk solution.

9. T4 Bacteriophage DNA Replication

DNA replication has been extensively studied in many different organisms because of its obvious physiological importance. The T4 bacteriophage DNA replication system is an excellent model system for the more complex systems found in eukaryotic cells. It has been extensively studied and reviewed.[46−48] All of the proteins involved have been purified and reconstituted with well-characterized DNA substrates. As shown schematically in Figure 8, DNA synthesis at the replication fork occurs on both the leading and lagging strands.

On the leading strand, the holoenzyme is formed by interaction of the DNA polymerase, gp43, with clamp (gp45) and clamp loader (gp44/62) proteins. The gp43 is positioned on the DNA template by the gp45 clamp, which is loaded onto the DNA by the clamp loader, with ATP being required for the loading process. Although DNA synthesis can occur with only gp43, the clamp proteins increase the processivity of the reaction. The gp43 also possesses a $3' \rightarrow 5'$ exonuclease activity that provides a proofreading mechanism. This activity can be removed from the gp43, thereby facilitating study of the polymerization reaction.

DNA replication on the lagging strand involves discontinuous synthesis of Okazaki fragments. Again gp43 is the

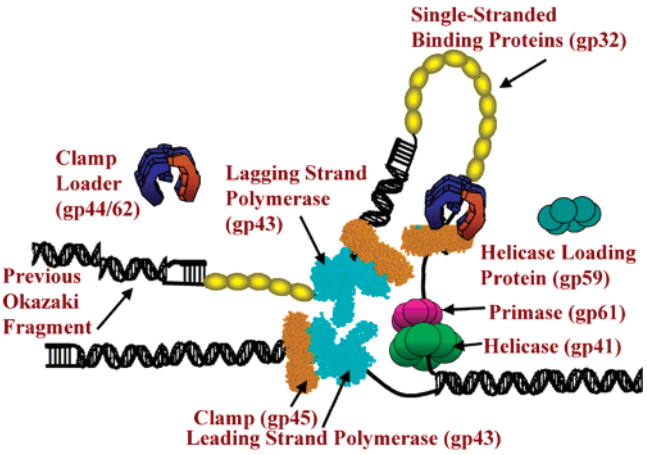

Figure 8. Cartoon of the bacteriophage T4 replisome. The cartoon illustrates replication on the leading and lagging strands of DNA and identifies the proteins involved. Figure courtesy of Dr. Stephen Benkovic, reprinted with permission. Copyright by Dr. Stephen Benkovic.

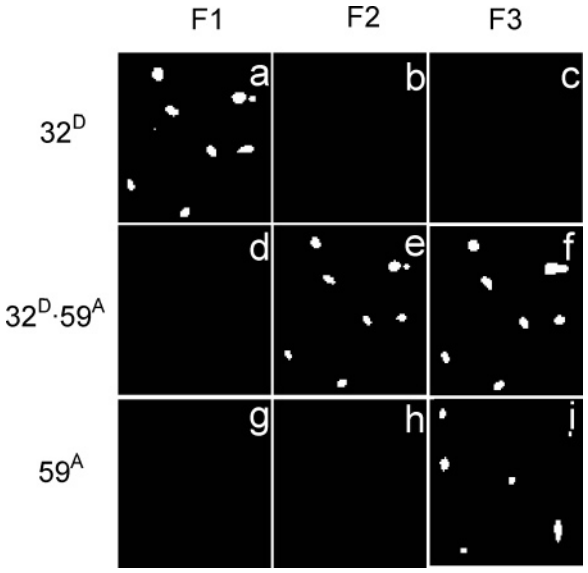

Figure 9. Fluorescence from individual molecules of forked DNA with the proteins bound in the order indicated. The gp32 is labeled with Alexa 488 (fluorescence donor), and the gp59 is labeled with Alexa 555 (fluorescence acceptor). The filter sets are described in the text. F1 detects Alexa 488 emission, F3 detects Alexa 555 emission, and F2 detects FRET between Alexa 488 and Alexa 555. Both proteins bind independently to the forked DNA. When both proteins are bound FRET occurs between the two proteins, indicating close association of gp32 and gp59. Background fluorescence has been removed with NIH Image software. Reprinted with permission from Z. Zhang, M. M. Spiering, M. A. Trakselis, F. T. Ishmael, J. Xi, S. J. Benkovic, and G. G. Hammes *Proc. Natl. Acad. Sci. U.S.A.* **2005**, *102*, 3254−3259. Correction **2005**, *102*, 13349−13351. Copyright 2005 National Academy of Sciences U.S.A.

DNA polymerase, but a primase, gp61, is needed to produce RNA primers. The group of proteins making the RNA is called the primosome whereas the entire group of proteins responsible for DNA synthesis is called the replisome. The Okazaki fragments are combined by a DNA ligase system. In order for the holoenzyme to advance through the DNA duplex, an ATP (or GTP) driven helicase (gp41) is required to unwind the duplex DNA. The lagging strand is coated with a single-strand binding protein, gp32, to prevent reannealing of the DNA, and an additional protein, gp59, is required to load some of the proteins onto the DNA and to regulate the overall process. Despite the complexity of the T4 replication systems, it is one of the simplest available for elucidation of the replication mechanism on a molecular basis. Well-characterized forked DNA substrates can be made, and the proteins can be labeled with fluorescent markers while still retaining biological activity.

The assembly of the primosome and replisome on the lagging strand has been studied with single molecule methods, and the role of gp59 in regulating DNA synthesis has been clarified.[49] Ensemble methods have not provided a clear-cut picture of these processes because the proteins involved interact both on and off the DNA, and it is difficult to unscramble these competing interactions. Furthermore, each DNA binds a different number of proteins. Both single-stranded and forked DNA molecules were synthesized with biotin at the 3′ or 5′ end so that they could be easily attached to the microscope slide. The forked DNA molecules have the appropriate structure so that both RNA and DNA can be synthesized. The proteins were labeled with either Alexa 488 or Alexa 555. FRET is possible between these probes, and the microscope was set up to observe fluorescence of Alexa 488 (filter set 1), FRET (filter set 2), or direct fluorescence of Alexa 555 (filter set 3). The various proteins were added to the slide containing the DNA by capillary action, and fluorescence was observed with an ICCD camera.

The primosome assembly on the lagging strand involves four proteins: gp32, gp59, gp41, and gp61. As shown in Figure 9, gp32 and gp59 each bind independently to DNA with essentially complete FRET. The stoichiometry of the protein binding to DNA is not absolute: different DNA molecules have a different number of proteins bound, as judged by the fluorescence intensity. Strictly speaking, this is not single molecule fluorescence: a single molecule of DNA binds multiple fluorescent proteins. The extensive FRET that occurs indicates the proteins interact closely. In the presence of MgATPγS (not hydrolyzed by gp41), gp41 binds weakly to the DNA coated with gp32 and gp59, with FRET occurring between gp59 and gp41. When MgATP is present, the results are initially the same, but after 30 min, the gp32 and gp59 are no longer bound to the DNA. The gp41, however, remains bound. The primase, gp61, binds only after gp41 binds. Extensive FRET occurs between bound gp41 and gp61, indicating that they interact closely. The gp41 binds to the DNA only when both gp32 and gp59 are present—neither one alone is sufficient. These results suggest that gp59 participates in the loading of gp41 onto DNA (gp59−gp41 FRET). The elimination of gp32 from the DNA (gp32−gp59 FRET) also requires the presence of gp59, because the helicase will not bind to DNA that has only gp32 bound to it. If gp32 and gp59 are both absent from the DNA, gp41 and gp61 both bind to DNA without the requirement of MgATP. However, this is a nonphysiological situation. Thus the final primosome contains only gp41 and gp61.

A cartoon of the primosome assembly mechanism is shown in Figure 10. The crystal structures of both gp32 and gp59 are known,[50,51] and cross-linking experiments have delineated the areas of interaction of gp59 with gp32 and gp41.[51] The gp32 and gp59 have been postulated to be hexameric when bound to the DNA, and gp41 is proposed to form a similar structure.

Ensemble experiments have shown that gp59 can completely inhibit both the polymerase and exonuclease activities.[52] Single molecule experiments have demonstrated that

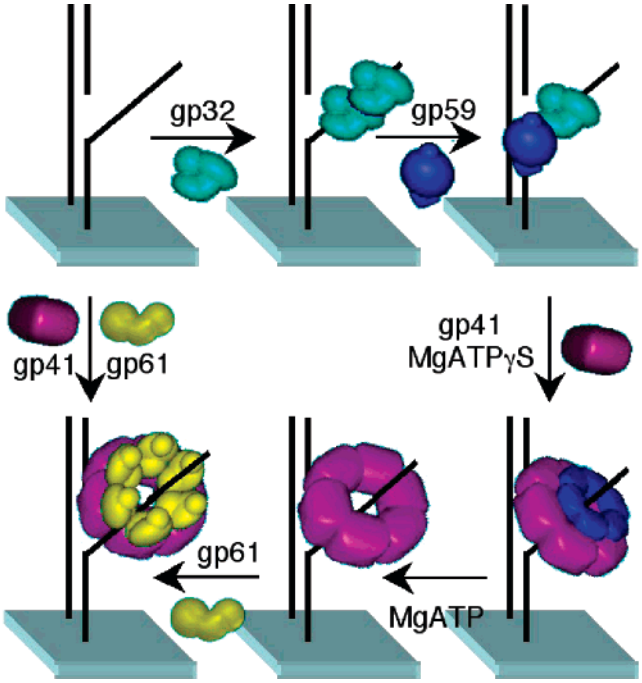

Figure 10. Cartoon of the assembly of the bacteriophage T4 lagging strand primosome to forked DNA. The gp32 protein binds to the DNA with either subsequent or concurrent binding of gp59. Then gp41 binds to gp59 and is loaded onto the DNA in the presence of nucleotide. MgATP hydrolysis is required for gp41 to displace gp32 and gp59, either directly or by translocation. Subsequently the gp61 protein binds and interacts closely with gp41 on DNA as judged by FRET. In the absence of gp32 and gp59, both gp41 and gp61 bind independently to DNA with MgATP hydrolysis not being required. Reprinted with permission from Z. Zhang, M. M. Spiering, M. A. Trakselis, F. T. Ishmael, J. Xi, S. J. Benkovic, and G. G. Hammes *Proc. Natl. Acad. Sci. U.S.A.* **2005**, *102*, 3254−3259. Correction **2005**, *102*, 13349−13351. Copyright 2005 National Academy of Sciences U.S.A.

this is due to a direct interaction between gp43 and gp59 on DNA: extensive energy transfer occurs between the two proteins when bound to DNA.[53] Furthermore, the residues of contact between the two proteins were established through chemical cross linking experiments and mass spectrometry. Molecular modeling suggests that the gp59 locks the gp43 into an inactive conformation. This interplay between single molecule and ensemble experiments has established the mechanism of inhibition unambiguously. These results also establish that assembly of the lagging strand polymerase can occur without leading strand polymerization even though leading and lagging strand polymerization are coordinated. The inhibition by gp59 can be unlocked by the addition of gp41 and MgATP.[54] Single molecule observations clearly demonstrate the loss of gp59 from the DNA when gp41 and MgATP are added to the "locked" replication system. A similar regulatory effect of gp59 has been recently observed in the intact phage system.[55]

Finally mention should be made of the fact that both DNA and RNA can be synthesized when the biotin-forked DNA is confined to a surface by the biotin−avidin interaction. RNA fragments have been detected, as has been the incorporation of fluorescent nucleotides into the forked DNA. Furthermore, the addition of nucleotide triphosphates to the single molecules containing primosomes and replisomes results in the loss of bound proteins.

In the case of T4 DNA replication, single molecule methods have provided an unambiguous way of monitoring

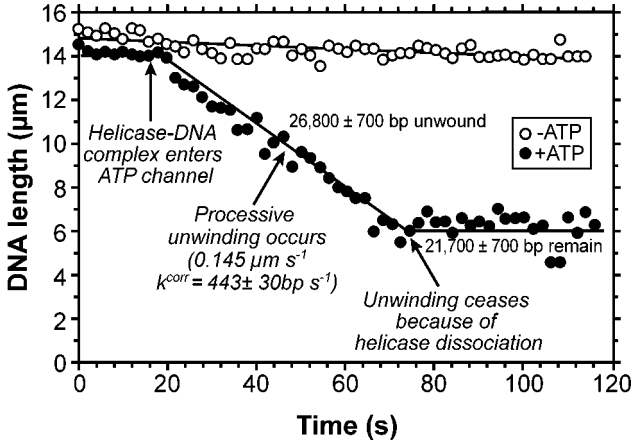

Figure 11. Unwinding of a λ DNA molecule by *Escherichia coli* RecBCD helicase. The DNA length in micrometers is plotted versus the time in seconds. The open circles are in the absence of ATP, and the closed circles are in the presence of ATP. The onset of unwinding can be seen at approximately 20 s, followed by a linear decrease in length. The unwinding stops when the helicase dissociates. Reprinted with permission from P. Blanco, L. R. Brewer, M. Corzett, R. Balhorn, Y. Yeh, and S. C. Kowalczykowski *Nature* **2001**, *409*, 374−378 (http://www.nature.com). Copyright 2001 Nature Publishing Group.

what is happening on a single DNA molecule, without the complication of what is happening in bulk solution. The coming and going of individual proteins can be visualized. Furthermore, these experiments have demonstrated the close interaction of specific proteins on the DNA through FRET. This has permitted the establishment of mechanistic features that were ambiguous in ensemble experiments. Future experiments examining holoenzyme formation on the leading strand and the kinetics of DNA polymerization should add further insight into the molecular mechanism of replication.

10. Helicases

Several single molecule studies have been directed at mechanistic aspects of helicases. RecBCD from *Escherichia coli* is a processive DNA helicase and nuclease that is involved in the repair of chromosomal DNA.[56] The translocation and DNA unwinding by a single DNA helicase molecule have been visualized by use of an optical trap. DNA substrates were constructed with biotin attached to one end of λ DNA. These DNA molecules were attached to streptavidin-coated polystyrene beads. A fluorescent dye was then bound to the DNA, followed by RecBCD in the absence of ATP. Under these conditions, the helicase binds only to the free end of the DNA, and translocation/unwinding does not occur until ATP is added. The DNA and ATP were placed in parallel flow paths. The flow-induced extension of the DNA from the bead, and the fluorescence of the extended DNA and the bead could be observed because of the nonspecific binding of fluorescent dye. Once the DNA−bead was trapped, it was moved to the flow boundary of the ATP channel, and the ATP caused helix unwinding. Since the RecBCD enzyme molecule is attached at an end opposite to the bead, DNA unwinding will proceed from the end opposite the bead toward the bead. This will appear in the microscope as an apparent decrease in the length of the DNA because the fluorescent dye is displaced by the enzyme as the duplex unwinds. This displacement was followed by a video camera with a time resolution of about 300 ms. The results of a typical experiment are shown in Figure 11.

These studies show that the unwinding is ATP-dependent and processive with up to 30 000 base pairs unwound before dissociation of the helicase. The processivity and rate of unwinding varied from molecule to molecule at a given ATP concentration—the variation was as great as a factor of 5. As expected, the rate and processivity increased with ATP concentration, approximately following saturation kinetics. The maximum processivity at 23 °C is about 30 000 base pairs per binding event with an apparent Michaelis constant for MgATP of about 160 μM. The maximum unwinding rate was found to be approximately 520 base pairs/s with an apparent Michaelis constant of 140 μM. These results are in good agreement with ensemble measurements. These data indicate that the unwinding process is continuous with no sequence specificity. However, the time resolution of the experiment is relatively long, so short stalls and base pair specificity may occur as the unwinding proceeds.

In a related study, the translocation of RecBCD on DNA was measured by binding single enzyme molecules to streptavidin-coated polystyrene beads.[57] These beads were placed above a glass surface with attached DNA molecules in the presence of DNA. The translocation process was measured by monitoring changes in Brownian motion of individual beads. This is a less direct method for observing the helicase−DNA interaction. However, the measured rate of translocation was similar to that reported above, a few hundred base pairs per second. Moreover, the enzyme translocation was found to be mostly unidirectional with a roughly constant velocity. No significant delay was found between the binding step and translocation.

The motion of RecBCD on DNA moving against applied forces also has been measured using optical trapping distance measurements, rather than fluorescence.[58] RecBCD molecules were attached to a streptavidin coated cover glass. The surface-tethered enzyme bound to one end of a 7.1 kilobase-pair double-stranded DNA, and the other end of the DNA was attached to a polystyrene bead that was held above the surface of the cover glass by an optical trap. (An optical trap focuses a laser on the bead, and the interaction of the light with the bead creates a pressure that holds the bead in place.) A force clamp was implemented through the servomotion of a piezoelectric operated stage, and movements along the DNA could be monitored by the stage motion to a detector limit of about 2 nm. Constant velocity motions per hundreds of thousand of base pairs were interrupted by sudden changes to different speeds or pauses of several seconds. Occasionally the RecBCD reversed its motion. These results are not directly comparable to the fluorescence experiments in which applied forces were not used. However, the results obtained show that RecBCD−DNA complexes exist in multiple functional states for many catalytic turnovers. This multiplicity of states may play a regulatory role in biological systems.

The studies discussed thus far use very large DNA and track the helicase over relatively long distances. Not all helicases are as processive as the RecBCD enzyme. To probe less processive helicases, the unwinding reaction catalyzed by the Rep helicase from *Escherichia coli* was examined.[59] The substrates were 18 base pair and 40 base pair DNA duplexes prepared with a 3′-$(dT)_{20}$ tail. A fluorescence donor (Cy3) and an acceptor fluorophore (Cy5) were attached at the junction between the single-stranded DNA and the double-stranded DNA. The DNA molecules are immobilized on the microscope slide and imaged. A solution was rapidly delivered to the DNA (<0.2 s) that contains the Rep helicase and ATP. Before unwinding begins, the donor and acceptor are sufficiently close that essentially complete FRET occurs. As unwinding occurs, the donor and acceptor move apart, and the FRET decreases. When unwinding is complete, the donor strand diffuses away, and the fluorescence signal disappears. As expected, ATP hydrolysis is necessary for unwinding. If the helicase concentration is very low, <2 nM, unwinding does not occur. Furthermore, above 20 nM helicase, time elapses before unwinding begins: this is attributed to the binding process.

For the 18 base pair molecule, DNA unwinding proceeds quickly to completion once initiated: the average time for unwinding events is about 0.4 s. The behavior of the 40 base pair DNA is more complex. Partial unwinding occurs, followed by stalls that persist for more than 1 s. In some cases, rewinding occurs, whereas in other cases unwinding continues. The model that emerges from a detailed analysis is that a monomer of the helicase binds to the single-stranded DNA tail and moves toward the junction with the duplex. Conformational fluctuations occur until either the monomer dissociates or an additional monomer binds to form a functional helicase. Unwinding then proceeds unless the functional helicase partially dissociates. Unwinding can resume when a functional helicase is formed. Rewinding can occur when the helicase completely dissociates from the DNA. Thus the observation of limited processivity for in vitro experiments is attributed to the instability of the active helicase. Whether this instability is an important physiological factor is not known. In principle, it could provide a regulatory mechanism for the unwinding process.

A related single molecule study has been carried out with UvrD, a DNA repair enzyme that unwinds duplex DNA while moving 3′ → 5′ on one strand.[60] In this case, a DNA molecule was bound at one end to a glass surface and at the other end to a small magnetic bead. The DNA was stretched by small magnets placed around the sample. The Brownian motion of the bead was measured to provide information about the molecular extension of the DNA. The actual parameter measured is the change in DNA length versus time as the DNA unwinds. Although this methodology is somewhat outside the purview of this review, it provides a means of measuring the rate, lifetime, and processivity of the enzymatic processes. Unlike ensemble assays, unwinding is followed by a rezipping of the separated strands that is limited by translocation of the enzyme between strands, rather than by dissociation of the enzyme. These results again suggest that the helicase mechanism may be more complex than revealed by ensemble measurements.

11. λ Exonuclease

Several single molecule studies have been directed toward the digestion of DNA by λ exonuclease. The first to utilize fluorescence attached biotinylated λ DNA to an avidin-coated coverslip.[61] The DNA was then straightened with a dc electric field. The single molecule of DNA was visualized by decorating it with a fluorescent dye that intercalated the DNA but did not affect the activity of the exonuclease. When the enzyme was added to the single DNA molecule, shortening of the DNA could be visualized by disappearance of the dye. The rate of digestion of the DNA was found to be about 1000 bases/s, and the reaction displayed high processivity: the decrease in the length of DNA was directly proportional to the time.

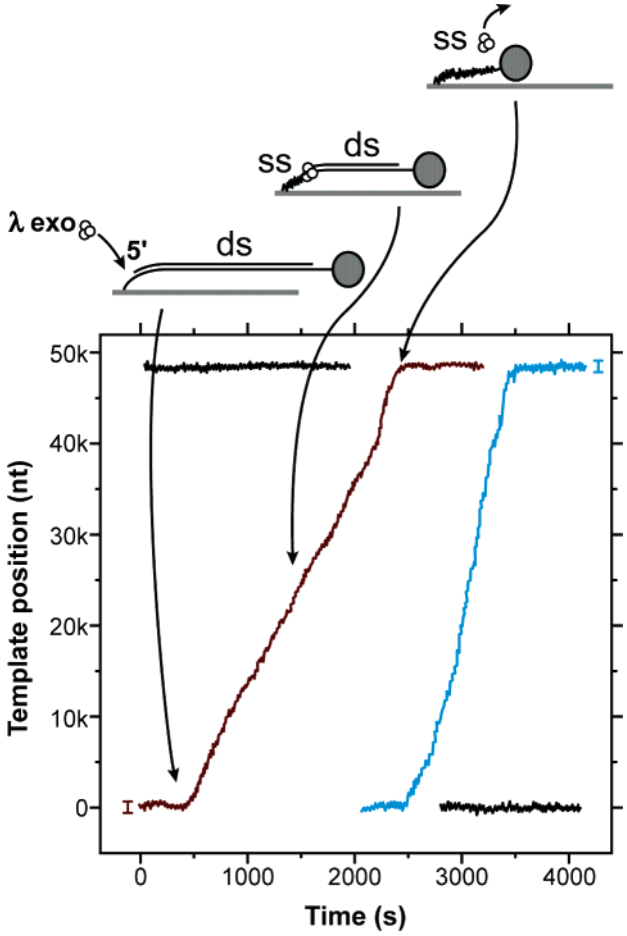

Figure 12. The time course for the digestion of two molecules of DNA by λ exonuclease. The template position versus time is plotted. Cartoons of the single stranded and double stranded DNA are shown above the plot for different regions of the trajectory. Reproduced with permission from A. M. van Oijen, P. C. Blainey, D. J. Crampton, C. C. Richardson, T. Ellenberger, and X. S. Xie *Science* **2003**, *301*, 1235−1238 (http://www.aaas.org). Copyright 2003 American Association for the Advancement of Science.

A somewhat different approach was taken by van Oijen et al.[28] Individual DNA molecules were attached at one end to a glass surface via a biotin−streptavidin interaction. The opposite end of the DNA was attached to polystyrene beads. Laminar flow was used to stretch the DNA, and the length of individual DNA molecules was determined by tracking the positions of the beads. The Brownian motion of the beads can be calibrated as a measure of the stretching force. Enzymatic digestion of the DNA at a constant stretching force causes a shortening of the DNA because single-stranded DNA is shorter than double-stranded DNA at low stretching forces. A typical time course for the digestion is shown in Figure 12. The λ nuclease initiates digestion at the 5′ end, and the DNA was designed so that only one such end was available, thus ensuring that only one molecule of enzyme bound to the DNA. The average number of base pairs converted to single-stranded DNA prior to dissociation of the enzyme, that is, the processivity, was found to be about 18 000 base pairs. The average rate of digestion was 32 nucleotides/s. These results were based on examining 44 DNA molecules, of which 4 were completely hydrolyzed.

The variation in rate among the single molecule trajectories suggested that digestion may be sequence dependent and that melting of the base pairs may be rate determining. In addition dynamic and/or static heterogeneity in the catalytic rates occurs. Although these conclusions are based on observation of a relatively small number of molecules, they are an indication of the unique information that can be obtained from single molecule experiments.

A single-molecule study of λ exonuclease also has been carried out using optical trapping and distance measurements.[62] In this work, a histidine-tagged derivative of the enzyme was attached to a cover glass coated with a histidine-specific antibody. A 7.1 kilo-base-pair double-stranded DNA was attached to the enzyme at one end and to a polystyrene bead at the other end. The bead was held in place above the cover glass by an optical trap. The digestion was initiated by the addition of Mg^{2+} and was monitored by maintaining the placement of the bead with a nanopositioning stage. The speed of digestion was nearly constant at 4 nm/s (about 12 nucleotides/s) with interspersed pauses of variable duration. The pauses occurred at strand-specific positions and were sequence dependent. The strongest pause was identified with the sequence GGCGA. These results complement those previously discussed and provide additional information about the molecular details of the reaction.

Although this review does not extensively consider the measurement of length changes in proteins and nucleic acids, mention of some related single molecule studies of RNA polymerase seems appropriate at this time. Bustamante's laboratory investigated the movement of RNA polymerase during transcription by attaching beads to the ends of a DNA molecule and stretching the DNA by flow.[63] The distance between beads can be directly measured by video microscopy and shortens as transcription occurs. Several significant features were noted. First, the rate of tether shortening varies for different molecules, that is, the transcription rate is variable. Second, each molecule shows a different propensity to pause and stop. Reversible pausing occurs during elongation, and eventually the enzyme stops permanently. The rate of transcription is not dependent on the stretching force over the range explored but depends on the nucleotide concentrations. The rate of transcription varied from a few base pairs per second to greater than 10 base pairs/s. In a later publication, optical trapping methods were used to probe the pausing and arresting during elongation when force was applied to individual transcribing molecules.[64] The translocation rate of the enzyme was not altered by the applied force, but the efficiency of pausing and arresting was affected.

In contrast to the above results, Adelman et al. found that the elongation kinetics were homogeneous among RNA molecules using optical trapping methodology.[65] The observed heterogeneity resulted from the variation in the frequency and duration of pausing. The discrepancy between these investigations remains to be resolved.

Block and co-workers also have used optical trapping to study the movement of RNA polymerase along a DNA template.[29,30] They were able to demonstrate that RNA polymerase may backtrack several bases. Moreover, backtracking pauses are enhanced under hindering loads and can be triggered by the misincorporation of noncomplementary nucleotides. By a significant technical improvement in the optical trapping methodology, they were able to achieve angstrom level resolution.[66] Discrete steps were observed averaging 3.7 Å, the mean rise per base pair in B-DNA. The RNA polymerase was concluded to advance along DNA by a single base pair per nucleotide addition to the nascent RNA. They were able to fit their results to a molecular model for

transcription that suggests movement is not tightly coupled to pyrophosphate release.

Obviously such an important enzyme merits more study at the single molecule level, and the use of fluorescence may enhance the molecular resolution.

12. HIV-1 Reverse Transcriptase

HIV-1 reverse transcriptase is responsible for transcribing viral RNA into double stranded DNA, with the DNA then being integrated into the host genome. The initial single molecule investigation of this enzyme merits special mention because equipment was developed that simultaneously measures the time dependence of the fluorescence intensity, fluorescence lifetime, and fluorescence anisotropy.[67] To carry out this study, a single cysteine on the enzyme was labeled with Alexa 488. A DNA/DNA primer/template was labeled with Cy5 at the 5′ end of the primer. The distance between the two probes was close to the Förster radius so that extensive energy transfer occurred. This condition maximizes the change in FRET that occurs as the distance between the energy donor and acceptor changes.

The enzymatic activity of the single molecules was directly observed by the addition of substrates and changes in FRET. Examination of single molecules of the DNA/DNA−enzyme complex indicated that three distinct species were present. The structures of two of these species are consistent with those observed with X-ray crystallography. Furthermore, the addition of nucleotide triphosphate or pyrophosphate suggested that they are the initially active state and product state in the polymerization reaction. The product state must undergo a conformational change before nucleotide incorporation can occur. The third structure is quite distinct: it does not incorporate nucleotides, and the nucleic acid substrate is bound at a site that is quite far from the nucleic acid binding tract revealed by X-ray crystallography. This was designated a dead-end complex.

Further single molecule studies of this system promise to shed additional light on the mechanism of action of the enzyme.

13. Conclusion

The work discussed here demonstrates that single molecule methodology is a useful tool to probe enzyme mechanisms. However, the importance of correlating single molecule experiments with ensemble studies to provide a coherent picture of mechanism is critical. An issue that remains to be resolved for single molecule studies is the role of the microenvironment. Is the static and/or dynamic disorder that has been observed of physiological relevance or a reflection of the surface localization? Or is it related to the limited number of events that can be observed for a single trajectory?

Even with these potential complications, new mechanistic information about enzyme function has been obtained. The method is particularly well suited for studying systems where complex arrays of proteins are required, for example, DNA polymerase. The organization and assembly of complex structures of proteins and nucleic acids can be determined unambiguously, without the interference of reactions/interactions occurring in the bulk solution and ensemble averaging. The examples discussed indicate the considerable potential of single molecule methods in this regard. Moreover, unique mechanistic information can be obtained without the complications of synchronization and ensemble averaging. Even assembled systems on membrane surfaces are good targets for investigation since lipids can be readily attached to glass surfaces.

Finally single molecule methods may reveal reaction intermediates that are transient or obscured in ensemble measurements. As the technology develops and becomes more routine, an increased number of mechanistic based studies can be anticipated.

14. Abbreviations Used

APD	avalanche photodiode
DHFR	dihydrofolate reductase
EMCCD	electron multiplying charge coupled device
FAD	flavin adenine dinucleotide
FMN	flavin mononucleotide
FRET	fluorescence resonance energy transfer
NADPH	nicotine adenine dinucleotide phosphate, reduced form
ICCD	intensified charge coupled device
TIRF	total internal reflection

15. Acknowledgment

This work was supported by National Institutes of Health Grant GM 65128.

16. Note Added in Proof

A review of single molecule studies of protein folding has recently appeared that includes an extensive discussion of single molecule FRET. Michalet, X.; Weiss, S. Jäger, M. *Chem. Rev.* **2006**, *106*, 1785.

17. References

(1) Special Issue on Single-Molecule Spectroscopy. *Acc. Chem. Res.* **2005**, *38*, 503−610.
(2) Weiss, S. *Science* **1999**, *283*, 1676.
(3) Li, H.; Ying, L.; Ren, X.; Balasubramanian, S.; Klenerman, D. *Biochem. Soc. Trans.* **2004**, *32*, 753.
(4) Xie, X. S.; Lu, H. P. *J. Biol. Sci.* **1999**, *274*, 15967.
(5) Ha, T. *Curr. Opin. Struct. Biol.* **2001**, *11*, 287.
(6) Greulich, K. O. *ChemPhysChem* **2005**, *6*, 2458.
(7) Brockelmann, U. *Curr. Opin. Struct. Biol.* **2004**, *14*, 368.
(8) Pierce, D. W.; Vale, R. D. *Methods Cell Biol.* **1999**, *58*, 49.
(9) Bai, L.; Santangelo, T. J.; Wang, M. D. *Annu. Rev. Biophys. Biomol. Struct.* **2006**, *35*, 343.
(10) Ha, T. *Biochemistry* **2004**, *43*, 4055.
(11) Coppin, C.; Finer, J.; Spudich, J. S.; Vale, R. *Biophys. J.* **1995**, *68*, 242S.
(12) Peterman, E. J. G.; Sosa, H.; Moerner, W. E. *Annu. Rev. Phys. Chem.* **2004**, *55*, 79.
(13) Capitanio, M.; Vanzi, F.; Broggio, C.; Cicchi, R.; Normanno, D.; Romano, G.; Sacconi, L.; Pavone, F. S. *Microsc. Res. Technol.* **2005**, *65*, 194.
(14) Yildiz, A.; Selvin, P. R. *Acc. Chem. Res.* **2005**, *38*, 574.
(15) Finer, J. T.; Simmons, R. M.; Spudich, J. A. *Nature* **1994**, *368*, 113.
(16) Ishijima, A.; Harada, Y.; Kojima, H.; Funatsu, T.; Higuchi, H.; Yanagida, T. *Biochem. Biophys. Res. Commun.* **1994**, *199*, 1057.
(17) Kinosita, K., Jr.; Adachi, K.; Itoh, H. *Annu. Rev. Biophys. Biomol. Struct.* **2004**, *33*, 245.
(18) Zhuang, X. W.; Bartley, L. E.; Babcock, H. P.; Russel, R.; Ha, T.; Herschlag, D.; Chu, S. *Science* **2000**, *288*, 2048.
(19) Tan, E.; Wilson, T. J.; Nahas, M. K.; Clegg, R. M.; Lilley, D. M.; Ha, T. *Proc. Natl. Acad. Sci. U.S.A.* **2003**, *100*, 9308.
(20) Zhuang, X.; Kim, H.; Pereira, M. J.; Babcock, H. P.; Walter, N. G.; Chu, S. *Science* **2002**, *296*, 1473.
(21) Bokinsky, G.; Zhuang, X. *Acc. Chem. Res.* **2005**, *38*, 566.
(22) Blanchard, S. C.; Kim, H. D.; Gonzalez, R. L., Jr.; Puglisi, J. D.; Chu, S. *Proc. Natl. Acad. Sci. U.S.A.* **2004** *101*, 12893.
(23) Axelrod, D. *Methods Cell Biol.* **1989**, *30*, 245.
(24) Magde, D.; Elson, E.; Webb, W. W. *Phys. Rev. Lett.* **1972**, *29*, 705.
(25) Lu, H. P.; Xun, L.; Xie, X. S. *Science* **1998**, *282*, 1877.
(26) Rajagopalan, P. T. R.; Zhang, Z.; McCourt, L.; Dwyer, M.; Benkovic, S. J.; Hammes, G. G. *Proc. Natl. Acad. Sci. U.S.A.* **2002**, *99*, 13481.

(27) Ha, T. *Methods* **2001**, *25*, 78.
(28) van Oijen, A. M.; Blainey, P. C.; Crampton, D. J.; Richardson, C. C.; Ellenberger, T.; Xie, X. S. *Science* **2003**, *301*, 1235.
(29) Neuman, K. C.; Abbondanzieri, E. A.; Landick, R.; Gelles, J.; Block, S. M. *Cell* **2003**, *115*, 437.
(30) Shaevitz, J. W.; Abbondanzieri, E. A.; Landick, R.; Block, S. M. *Nature* **2003**, *426*, 684.
(31) Ha, T.; Ting, A. Y.; Liang, J.; Caldwell, W. B.; Deniz, A. A.; Chemla, D. S.; Schultz, P. G.; Weiss, S. *Proc. Natl. Acad. Sci. U.S.A.* **1999**, *96*, 893.
(32) Funatsu, T.; Harada, Y.; Tokunaga, M.; Salto, K.; Yanagida, T. *Nature* **1995**, *374*, 555.
(33) Schenter, G. K.; Lu, H. P.; Xie, X. S. *J. Phys. Chem. A* **1999**, *103*, 10477.
(34) Xie, S. *Single Mol.* **2001**, *4*, 229.
(35) Kou, S. C.; Cherayil, B. J.; Min, W.; English, B. P.; Xie, X. S *J. Phys. Chem. B* **2005**, *109*, 19068.
(36) Russel, R. University of Texas, Austin, personal communication.
(37) Yang, H.; Luo, G.; Karnchanaphanurach, P.; Louie, T.; Rech, I.; Cova, S.; Xun, L.; Xie, X. S. *Science* **2003**, *302*, 262.
(38) Shi, J.; Palfey, B. A.; Dertouzos, J.; Jensen, K. F.; Gafni, A.; Steel, D. *J. Am. Chem. Soc.* **2004**, *126*, 6914.
(39) Brendor, J. R.; Dertouzos, J.; Ballou, D. P.; Massey, V.; Palfey, B. A.; Entsch, B.; Steel, D. G.; Gafni, A. *J. Am. Chem. Soc.* **2005**, *127*, 18178.
(40) Zhang, Z.; Rajagopalan, P. T. R.; Selzer, T.; Benkovic, S. J.; Hammes, G. G. *Proc. Natl. Acad. Sci. U.S.A.* **2004**, *101*, 2764.
(41) Antikainen, N. M.; Smiley, R. D.; Benkovic, S. J.; Hammes, G. G. *Biochemistry* **2005**, *44*, 16835.
(42) Agarwal, P. K.; Billeter, S. R.; Rajagopalan, P. T. R.; Benkovic, S. J.; Hammes-Schiffer, S. *Proc. Nat. Acad. Sci. U.S.A.* **2002**, *99*, 2794.
(43) Chen, Y.; Hu, D.; Vorpagel, E. R.; Lu, H. P. *J. Phys. Chem. B* **2003**, *107*, 7947.
(44) Flomenbom, O.; Velonia, K.; Loos, D.; Masuo, S.; Cotlet, M.; Engelborghs, Y.; Hofkens, J.; Rowan, A. E.; Nolte, R. J. M.; Van der Auweraer, M.; de Schryver, F. C.; Klafter, J. *Proc. Natl. Acad. Sci. U.S.A.* **2005**, *102*, 2368.
(45) Edman, L.; Foldes-Papp, Z.; Wennmalm, S.; Rigler, R. *Chem. Phys.* **1999**, *247*, 11.
(46) Alberts, B. M. *Philos. Trans. R. Soc. London, Ser. B* **1987**, *317*, 395.
(47) Nossal, N. G. *Molecular Biology of Bacteriophage*; ASM Press: Washington, DC, 2001; p 43.
(48) Benkovic, S. J.; Valentine, A. M.; Salinas, F. *Annu. Rev. Biochem.* **2001**, *70*, 181.
(49) Zhang, Z.; Spiering, M. M.; Trakselis, M. A.; Ishmael, F. T.; Xi, J.; Benkovic, S. J.; Hammes, G. G. *Proc. Natl. Acad. Sci. U.S.A.* **2005**, *102*, 3254.
(50) Mueser, T. C.; Jones, C. E.; Nossal; N. G., Hyde, C. C. *J. Mol. Biol.* **2000**, *296*, 597.
(51) Shamoo, Y.; Friedman, A. M.; Parsons, M. R.; Konigsberg, W. H.; Steitz, T. A. *Nature* **1995**, *376*, 362.
(52) Ishmael, F. T.; Alley, S. C.; Benkovic, S. J. *J. Biol. Chem.* **2001**, *276*, 25236.
(53) Xi, J.; Zhuang, Z.; Zhang, Z.; Selzer, T.; Spiering, M. M.; Hammes, G. G.; Benkovic, S. J. *Biochemistry* **2005**, *44*, 2305.
(54) Xi, J.; Zhang, Z.; Zhuang, Z.; Yang, J.; Spiering, M. M.; Hammes, G. G.; Benkovic, S. J. *Biochemistry* **2005**, *44*, 7747.
(55) Dudas, K. C.; Kreuzer, K. *J. Biol. Chem.* **2005**, *280*, 21561.
(56) Bianco, P. R.; Brewer, L. R.; Corzette, M.; Balhorn, R.; Yeh, Y.; Kowalczykowski, S. C.; Baskin, R. J. *Nature* **2001**, *409*, 374.
(57) Dohoney, K. M.; Gelles, J. *Nature* **2001**, *409*, 370.
(58) Perkins, T. T.; Li, H.-W.; Dalal, R. V.; Gelles; Block, S. M. *Biophys. J.* **2004**, *86*, 1640.
(59) Ha, T.; Rasnik, I.; Cheng, W.; Babcock, H. P.; Gauss, G. H.; Lohman, T. M.; Chu, S. *Nature* **2002**, *419*, 638.
(60) Dessinges, M. N.; Lionnet, T.; Xi, X. G.; Bensimon, D.; Croquette, V. *Proc. Natl. Acad. Sci. U.S.A.* **2004**, *101*, 6439.
(61) Matsuura, S.; Komatsu, J.; Hirano, K.; Yasuda, H.; Takashima, K.; Katsura, S.; Mizuno, A. *Nucleic Acids Res.* **2001**, *29*, 79.
(62) Perkins, T. T.; Dalai, R. V.; Mitsis, P. G.; Block, S. M. *Science* **2003**, *301*, 1914.
(63) Davenport, R. J.; Wuite, G. J. L.; Landick, R.; Bustamante, C. *Science* **2000**, *287*, 249.
(64) Forde, N. R.; Izhaky, D.; Woodcock, G. R.; Wuite, G. J. L.; Bustamante, C. *Proc. Natl. Acad. Sci. U.S.A.* **2002** *99*, 11682.
(65) Adelman, K.; La Porta, A.; Santangelo, T. J.; Lis, J. T.; Roberts, J. W.; Wang, M. D. *Proc. Natl. Acad. Sci. U.S.A.* **2002** *99*, 13538.
(66) Abbondanzieri, E. A.; Greenleaf, W. J.; Shaevitz, J. W.; Landick, R.; Block, S. M. *Nature* **2005** *438*, 460.
(67) Rothwell, P. J.; Berger, S.; Kensch, O.; Felekyan, S.; Antonik, M.; Wohrl, B. M.; Restle, T.; Goody, R. S.; Seidel, C. A. M. *Proc. Natl. Acad. Sci. U.S.A.* **2003**, *100*, 1655.

CR0502955